Heliyon 6 (2020) e04347

Contents lists available at ScienceDirect

Heliyon

journal homepage: www.cell.com/heliyon

Research article

Local SDF-1α application enhances the therapeutic efficacy of BMSCs transplantation in osteoporotic bone healing

Qian Liu [a,1], Yi Wen [a,1], Jun Qiu [b,1], Zhaoyichun Zhang [b], Zuolin Jin [a], Meng Cao [a], Yang Jiao [c,**], Hongxu Yang [b,*]

[a] State Key Laboratory of Military Stomatology & National Clinical Research Center for Oral Disease & Shaanxi Key Laboratory of Oral Disease, Department of Orthodontics, School of Stomatology, The Fourth Military Medical University, Xi'an, China
[b] State Key Laboratory of Military Stomatology & National Clinical Research Center for Oral Diseases & Shaanxi International Joint Research Center for Oral Diseases, Department of Oral Anatomy and Physiology and TMD, School of Stomatology, The Fourth Military Medical University, Xi'an, China
[c] Department of Stomatology, The 7th Medical Center of PLA General Hospital, Beijing, China

ARTICLE INFO

Keywords:
Osteoporosis
Bone defects
BMSCs
SDF-1α
Osteogenesis
Regeneration
Biochemistry
Cell differentiation
Musculoskeletal system
Oral medicine
Periodontics
Regenerative medicine
Stem cells research

ABSTRACT

Bone defect healing is markedly impaired in osteoporotic patient due to poor bone regeneration ability. Stromal cell derived factor-1α (SDF-1α) plays a pivotal role in the repair of various injured tissues including bone. Here, we definite that SDF-1α hydrogels potentiates *in vivo* osteogenesis of bone marrow-derived stromal stem cells (BMSCs) in osteoporosis. The characteristics of rat primary BMSCs including superficial markers by flow cytometry and multi-lineage differentiation by induction were determined. At different time intervals, the release media from the SDF-1α-releasing hydrogels were collected to identificate SDF-1α exhibited a sustained release profile and maintained its bioactivity after release from the hydrogels to stimulate chemotaxis of BMSCs in a time dependent manner. Bilateral alveolar defects were operated in ovariectomized (OVX) rats and repaired with systemic BMSCs transplantation with or without the hydrogels. Local administration of SDF-1α significantly enhanced BMSCs recruitment and promoted more bone regeneration as well as the expression of OCN and Runx2 compared with the effect of BMSCs transplantation alone. Moreover, after BMSCs transplantation with SDF-1α delivery, macrophage polarization was promoted toward the M2 phenotype, that is identified as an important symbol in tissue regeneration process. Taken together, local SDF-1α application enhances the efficacy of BMSCs transplantation therapy in osteoporotic bone healing, suggesting clinical potential of SDF-1α to serve as a therapeutic drug target for osteoporosis treatment.

1. Introduction

Alveolar bone defects caused by periodontal diseases are still unclear for clinicians and researchers [1]. Postmenopausal osteoporosis is one of the most common and severe skeletal disorders over the world which the patients face increased risks of fractures, bone defects and alveolar bone resorption [2]. Moreover, ovariectomized (OVX)-osteoporosis negatively affects the healing process of both long and alveolar bones [3, 4]. Although bone marrow-derived mesenchymal stem cells (BMSCs) are the primary cells responsible for regulating bone metabolism and maintaining bone homeostasis, their regenerative ability is significantly impeded in patients with postmenopausal osteoporosis due to estrogen deficiency and inflammation environment [5].

Systemic mesenchymal stem cell transplantation (MSCT) has been successfully used for disease treatment and tissue regeneration. A lot of therapeutic mechanisms and materials may contribute to MSCT-based therapies including direct participation of MSCs in new tissues, paracrine secretion of cytokines and interplay between MSCs and immune cells [6]. BMSCs have been widely used in tissue repair or regeneration due to their self-renewal potential and multi-differentiation capability [7]. Compared with localized administration of BMSCs, systemic BMSCT simplifies clinical administration technique and improves cell survival rate *in vivo* by injecting cells into nutrient- and oxygen-rich vessels [8].

* Corresponding author.
** Corresponding author.
E-mail addresses: jiaoyang1989731@163.com (Y. Jiao), hxyang@fmmu.edu.cn, yanghongxushmily@163.com (H. Yang).
[1] These authors contributed equally to this work and should be considered co-first authors.

https://doi.org/10.1016/j.heliyon.2020.e04347
Received 11 March 2020; Received in revised form 22 May 2020; Accepted 25 June 2020

Exciting research confirmed that the systemic BMSCT to bone regeneration and remodeling could have a high effect treatment of osteoporosis [9, 10]. Unfortunately, poor engraftment of transplanted cells due to cell loss via blood circulation has been the major challenge of this therapy system [11].

Stromal cell-derived factor-1α (SDF-1α) as well as its receptor C-X-C chemokine receptor type 4 (CXCR4) has engendered increasing levels of attention in the regenerative medicine community [12]. Previous studies indicated that SDF-1α plays a pivotal role in bone repair and tissue regeneration by recruiting circulating or residing CXCR4-positive MSCs including BMSCs to the injury site [13]. The improvement of SDF-1α/CXCR4 axis for bone defect repair and orthodontic tooth movement seems important [14, 15, 16]. Our previous study demonstrated that pre-treatment with SDF-1α enhanced the proliferation, migration and differentiation of BMSCs derived from normal and postmenopausal osteoporotic rats *in vitro* [5]. Chitosan-based hydrogels are preferentially selected systems for drug and antibody delivery or tissue engineering scaffolds because of their beneficial qualities such as good biodegradability sustained release of drugs, biocompatibility and 3D hydrophilic polymeric networks [17]. However, the effects of local SDF-1α hydrogels administration *in vivo* on stem cell recruitment and bone defect repair in osteoporosis have not been elucidated.

In this study, we first investigated the effect of SDF-1α hydrogels on BMSCs *in vitro* and local administration of SDF-1α plays a key role in the therapeutic efficacy of BMSCT for osteoporotic bone regeneration in an OVX rat alveolar bone defect model. Moreover, after BMSCs transplantation with SDF-1α delivery, we revealed the macrophage polarization toward the M2 phenotype which is considered as an important promoting factor in tissue regeneration. Herein, we provided a new potential application of SDF-1α for treating the bone healing process in osteoporotic individuals.

2. Materials and methods

2.1. Animals

All procedures were approved by the Ethics Committee of the Fourth Military Medical University (SYXK2019-010, Xi'an, China), which meet the NIH and ARRIVE guidelines for the care and use of laboratory animals. Experiments were performed on sixty female Sprague Dawley (SD) rats aged 12 weeks and weighting 200 ± 20 g (Laboratory Animal Center, Fourth Military Medical University, China). Sham surgery and bilateral surgical ovariectomy (OVX) were performed by dorsal approach under general anesthesia to establish OVX-induced osteoporosis model as described previously [18, 19]. All animals were housed under specific pathogen-free conditions with free access to food and water.

2.2. Isolation and characterization of BMSCs

BMSCs were isolated from seven female SD rats and characterized with regard to their expression of surface markers and multi-lineage differentiation, as reported in our previous studies [5, 18, 19]. After sacrificed, bone marrow tissue was washing out from the femur and tibia. The tissues were incubated in α-minimum essential medium (α-MEM; Hyclone, USA) which contained with 20% fetal bovine serum (FBS; Hyclone, China) and 1% penicillin and streptomycin (Gibco, USA) in 10-cm diameter wells. BMSCs at passages 2–3 were used for the following experiments. Surface marker CD 29, CD34, CD 44, CD45, CD90, or CD105 (BD Bioscience, USA) were detected with a Beckman Coulter EpicsXL cytometer (Beckman Coulter, USA). Osteogenic and adipogenic differentiation assays were used to confirm the multiple differentiation potentials of rat BMSCs [19]. The cells were incubated for 2 weeks for the osteogenic differentiation assay or 3 weeks for the adipogenic differentiation assay, and the medium was refreshed every 3 days for both assays. Finally, the resultant mineralized cell nodules were characterized by Alizarin Red S staining, and the resultant lipid droplets were characterized by Oil Red O staining. Images were taken by the inverted microscope (Olympus, Japan).

2.3. Preparation of chitosan-based hydrogels

Chitosan/β-glycerolphosphate/hydroxyethyl cellulose (CS/GP/HEC) hydrogels were prepared as previously described protocol [20]. Firstly, 0.2 g CS (Sigma-Aldrich, USA) was added in 8 mL acetic acid solution (0.1 M). Then GP solution, which was prepared by dissolving 0.56 g of GP (Sigma-Aldrich, USA) in 2 ml of distilled water, was added into the stirring CS solution. Subsequently, SDF-1α (Peprotech, USA) at 100 ng/ml was homogeneously re-suspended in the HEC solution, which was prepared by dissolving HEC (Sigma-Aldrich, USA) at 20 mg/mL in α-MEM. The two solutions were sterilized by microfiltration and mixed by adding 0.2 ml HEC SDF-1α drop-wise into 0.8 ml CS/GP solution at 37 °C for 15 min. The mixture was planted in a 6-well plate for 30 min for gelation. All procedures were performed under aseptic conditions. The hydrogels were subsequently stored at -20 °C for further experiments.

2.4. In vitro SDF-1α release kinetics

To evaluate the release kinetics of SDF-1α, 1 ml PBS (pH = 7.4) was added over the SDF-1α/hydrogels. The hydrogels were incubated in 37 °C with a shaker. At different time-point groups, samples and PBS were taken out for further detecting. The SDF-1α concentrations in the collected PBS were quantified using an ELISA kit (Elabscience, China) by the protocol. The cumulative release ratio was calculated as the ratio of the cumulative mass of SDF-1α released at each time interval to their initial input amount in the hydrogels.

2.5. Transwell migration assay

The release of SDF-1α from SDF-1α/hydrogels and its bioactivity property was detected by the migration assay through a transwell plate [5]. Briefly, 1×10^5 BMSCs were seeded onto the upper case of a transwell plate (Corning, USA). The SDF-1α/hydrogels which were contained with 1 mL of α-MEM medium were prepared. These mediums were collected at the different experiment time points, while hydrogels were prepared as the control group. Then the release media were added into the lower case of transwell separately. 3, 6, 9 days later, the migrating cells from the upper case to lower case in transwell were collected. The migrated cells number was counted by double blind evaluations.

2.6. Surgical procedures

The rat alveolar bone defect models were established as our previous studies [21]. The surgical sample was selected as the distal to the maxillary first molar on right side. The alveolar bone defect was prepared with round burs to remove bone tissue (Mani, Japan), compared with copious saline irrigation to keep low temperature at the area of defect. We created a defect of approximately 4 × 3 × 3 mm (Figure 1). Five SD rats used in Blank Control group 0 week (after establish bone defect) for the detection of micro-CT. Twenty-four SD rats randomly assigned into three groups; im-BMSCs group (implantation of BMSCs) received the implantation of BMSCs into defect and im-BMSCs + SDF-1α-Hy group (implantation of BMSCs with SDF-1α hydrogels) received the implantation of BMSCs into defect combined with local pure SDF-1α-hydrogel grafts, respectively; PBS was used to inject into the bone defect as Blank Control (n = 8; 5 for micro-CT and sample sections, 3 for qRT-PCR and Western blotting assays in every groups). 8 weeks after transplantation, the rats were sacrificed and sampled.

To detect the homing of administrated BMSCs, the cells were labelled with a cell tracer CM-Dil (Invitrogen, USA) before injection [19]. The labeled BMSCs were re-suspended in saline at a concentration of 1×10^7 cells/mL. 500 μL BMSCs saline were then injected intravenously into three groups (Blank Control group, im-BMSCs group and im-BMSCs +

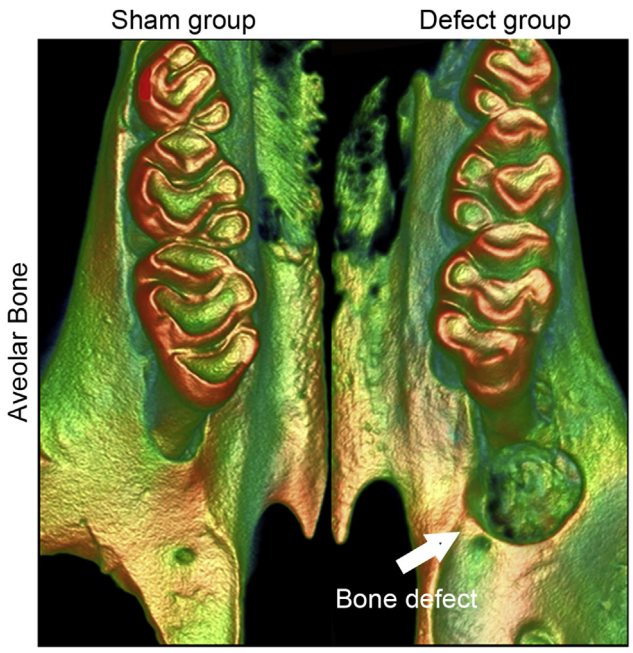

Figure 1. Representative image of the alveolar bone defects beside the first molar. The aim of the procedure was to create an alveolar bone defect of approximately 4 × 3 × 3 mm.

SDF-1α-Hy group) respectively via tail vein at another twenty-four SD rats (n = 8; 5 for micro-CT and sample sections, 3 for qRT-PCR in every groups) [22]. 8 weeks after injection, the rats were sacrificed and sampled.

2.7. Micro-CT analysis

The Inveon micro-CT system (Siemens AG, Germany) was applied to scan the maxillae samples with a source voltage of 80 kV, current of 500 μA and 14.97 mm isotropic resolution. Images of the defects were reconstructed and analyzed using parameters of Hounsfield Unit (HU) value, bone mineral density (BMD), BV/TV and Tb.Th with Inveon Research Workplace (Inveon, Siemens, Germany).

2.8. Histological and immunofluorescence staining

After Micro-CT analysis, bone samples were harvested, fixed in 4% paraformaldehyde and then decalcified with 10% EDTA, followed by paraffin or optimal cutting temperature compound (OCT; Sakura Finetek, USA) embedding. The sections were stained with hematoxylin-eosin (H&E) staining, Masson's trichrome (MT) staining, respectively. Immunofluorescence staining for Osteocalcin (OCN, ab13420, 1:100; Abcam), Runx2 (ab23981, 1:100; Abcam) and 4,6-diamidino-2-phenylindole (DAPI; Beyotime, China) were then performed in the sections from each group after tail vain injection experiments. All images were obtained with a confocal laser scanning microscope (FV1000; Olympus, Japan).

2.9. Western blot and qRT-PCR analysis

Bone samples in the new bone formation regions and cervical lymph nodes for each group were immediately frozen in liquid nitrogen and stored at -80 °C after the rats were sacrificed. The total protein and RNA was extracted with Tripure reagent (Roche, Germany) [21]. The protein samples (20 μg) were resolved on 10% SDS-PAGE gels, transferred onto nitrocellulose membranes (Bio-Rad, Hercules, CA, USA) at 4 °C and 300 mA for 1 h and then blocked with 5% nonfat milk for 1 h. The PVDF membranes were incubated with primary antibodies overnight at 4 °C for anti-ALP antibody (ab83259, Abcam, Cambridge, UK), anti-BMP1 antibody (ab205394, Abcam, Cambridge, UK) and anti-COL-1 antibody (146951-1AP, Proteintech, Cambridge, UK). After rinsing, the membrane was incubated with horseradish peroxidase (HRP)-conjugated IgG secondary antibodies (Zhongshan Golden Bridge, Xi'an, China). Protein bands were detected using an enhanced chemiluminescence (ECL) system (Bio-Rad).

500 ng total RNA of each sample was transcribed into cDNA by a PrimeScript RT reagent kit (TaKaRa, Japan). The analysis of expression was performed on the CFX96^{TM} Real Time RT-PCR System with SYBR PremixExTaq^{TM} II (TaKaRa, Japan) according to the manufacturer's instructions. The relative gene expression was determined using the $^{\Delta\Delta}$Ct method. The primer sequences are provided in Table 1. Glyceraldehyde 3-phosphate dehydrogenase (*Gapdh*) was used to normalize the expression level of related genes.

2.10. Statistical analysis

All values are presented as the mean ± standard deviation (SD) from at least three independent experiments. Comparisons were performed by two-tailed Student's t-test (for two-group analysis) or one-way analysis of variance (ANOVA) followed by the Newman-Keuls post-hoc tests (for multiple group analysis) using SPSS 21.0 (SPSS Inc, USA). Significance was confirmed at $P < 0.05$.

3. Results

3.1. Characterization of BMSCs and sustained release of bioactive SDF-1α from the hydrogels

Flow cytometry analysis demonstrated that the BMSCs from rat were positive for various mesenchymal-associated markers, including CD29, CD44, CD90 and CD105, and negative for hematopoietic markers, including CD34 and CD45 (Figure 2A). After osteogenic and adipogenic induction, Alizarin Red and Oil Red O staining illustrated the significant differentiation potential of the isolated BMSCs (Fig. 2B, C). Then, the cumulative release profiles of SDF-1α were detected. There was a burst release with 55% of the total SDF-1α released from the hydrogels in the first 3 days, then reached to 96% at day 21 (Figure 2D). The bioactivity of SDF-1α released from the hydrogels on migration of BMSCs were collected at 3, 6 and 9 days. The SDF-1α bioactivity significantly increased cell migration in a dose-dependent manner after release from the hydrogels (Fig. 2E, F).

3.2. Effect of SDF-1α on alveolar bone defect repair in OVX rats

The new bone formation was reconstructed by micro-CT imaging at 8 weeks post-surgery. Micro-CT analysis showed almost complete repair of the bone defect in the im-BMSCs + SDF-1α-Hy group, whereas the defect in the Blank Control group showed no evidence of healing (Figure 3A). Significant increases in bone volume and BMD were observed in the im-BMSCs + SDF-1α-Hy group compared with the im-BMSCs group and Blank Control group (Fig. 3B, C). Moreover, the values of BV/TV and Tb.Th upregulated in the im-BMSCs + SDF-1α-Hy group (Fig. 3D, E). For histological staining, very little new bone formation was observed but almost only connective tissue in the defect area in the Blank Control group. The defect area in the im-BMSCs group was filled with osteoblasts or osteogenetic cells and connective tissues as well as a small quantity of new bones. However, the im-BMSCs + SDF-1α-Hy group showed better healing results with compacted trabecular pattern and vascular structures in the newly formed bones (Figure 4A). Masson staining revealed that there was more new bone and fibers in the im-BMSCs + SDF-1α-Hy group than the im-BMSCs group (Fig. 4B, C). The same trend was observed in the protein expression levels of ALP, BMP1 and COL-1 by Western blot (Fig. 4D, E). In short, we confirmed that the combined treatment group had the best regeneration effect among these groups.

Table 1. Primer sequences.

Gene	Forward	Reverse
Runx2	5′-GCCACCTTCACTTACACCCC-3′	5′-GAGATGATACCATGAAGCAGTCGC -3′
Ocn	5′-AGACTCCGGCGCTACCTCAACAAT-3′	5′-TCATACCTGCCGTGTCGAC -3′
Cxcr4	5′-CCTCCTCCTGACTATCCCTGA-3′	5′-GTTCGTTCCTACACTCAAGC -3′
IL-1β	5′-AGGCTGACAGACCCCAAAAG-3′	5′-CTCCACGGGCAAGACATAGG-3′
TNF-α	5′-GATCGGTCCCAACAAGGAGG-3′	5′-TTTGCTACGACGTGGGCTAC-3′
iNOS	5′-TATCTGCAGACACATACTTTACGC-3′	5′-TCCTGGAACCACTCGTACTTG-3′
CD206	5′-GACGGACGAGGAGTTCATTATAC-3′	5′-GTTGGAGAGATAGGCACAGAAG-3′
IL-10	5′-CCTCTGGATACAGCTGCGAC-3′	5′-TGAGTGTCACGTAGGCTTCT-3′
Arg1	5′- GAACACGGCAGTGGCTTTAAC-3′	5′-TGCTTAGCTCTGTCTGCTTTGC-3′
Gapdh	5′-GGAAACCCATCACCATCTTC-3′	5′-TGAGTCTTCTGACACCTACCG-3′

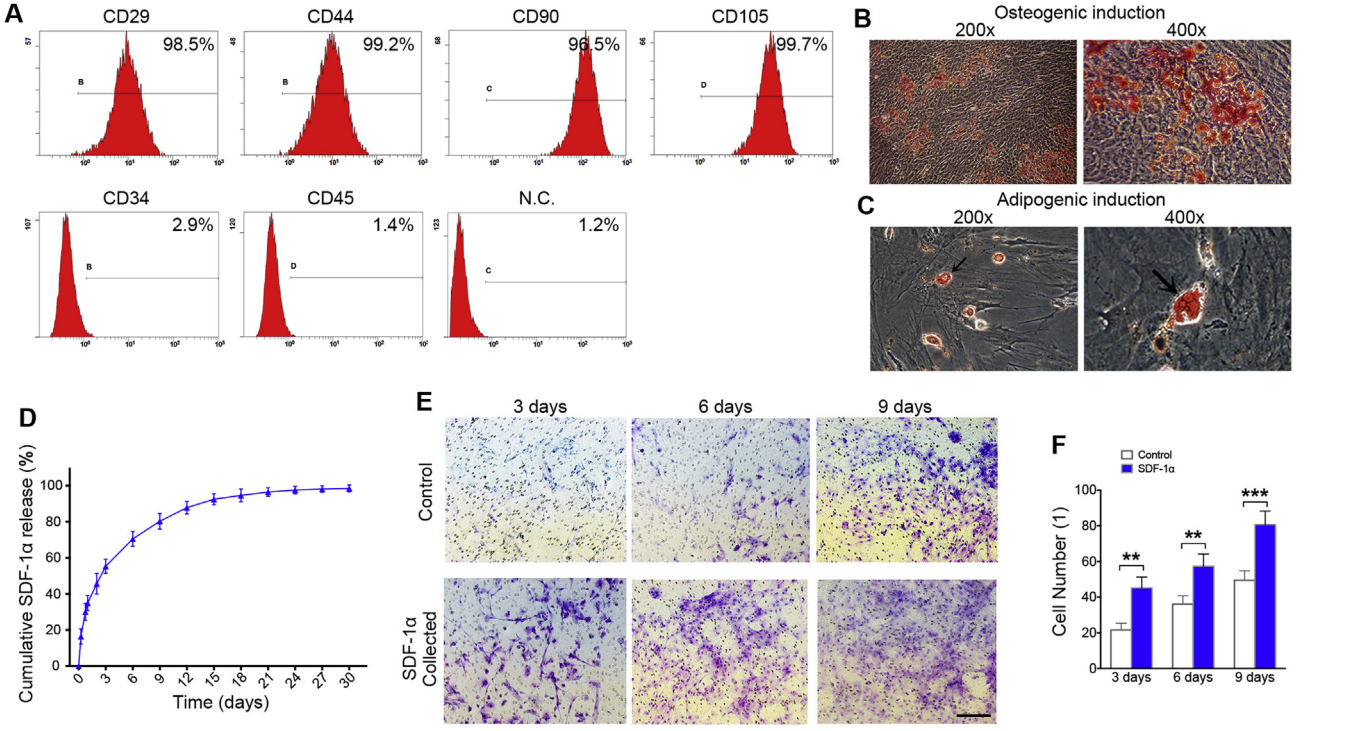

Figure 2. Characterization of BMSCs and SDF-1α/CS/GP/HEC hydrogels provide sustained release of bioactive SDF-1α. (A) Flow cytometric analysis of BMSCs surface markers for CD29, CD44, CD90, CD105, CD34 and CD45. (B) BMSCs cultured in osteogenic induced media, mineralized nodules detected by Alizarin Red staining. (C) Cultured BMSCs formed Oil Red O-positive lipid droplets of adipogenic induction. Black arrow, lipid droplets. (D) SDF-1α release from SDF-1α/CS/GP/HEC hydrogels is sustained over 30 days *in vitro*. (E) Migration of BMSCs in response to the release media collected at 3, 6 and 9 days in a transwell assay. (F) The migrated cell number of BMSCs in release media. Data are presented as mean ± SD. n = 3. $^{**}p < 0.01$, $^{***}p < 0.001$ represent significant differences.

3.3. Effect of SDF-1α on polarization states during bone regeneration

The interplay between BMSCs and immune cells has been recognized as a significant principle for BMSCT therapy. Thus, the polarization states of the macrophages in the cervical lymph nodes were analyzed by qRT-PCR analysis. The results showed that the expression levels of *IL-1β*, *TNF-α* and *iNOS* genes, which were related to macrophage polarization toward the M1 phenotype, was significantly downregulated in the two experiment groups compared with the Blank Control group; the lowest expression levels of these genes were observed in the im-BMSCs + SDF-1α-Hy group (Figure 4F). In contrast, the expression levels of *CD206*, *IL-10* and *Arg1* genes, which were related to M2 phenotype in macrophage polarization process, was significantly increased in the two experiment groups compared with the control group, especially in the im-BMSCs + SDF-1α-Hy group (Figure 4G). These results suggested SDF-1α delivery during BMSCs transplantation exerted an additive effect on macrophage polarization to promote bone regeneration.

3.4. Effect of SDF-1α on BMSCs recruitment and osteogenesis in vivo

To detect the homing of administrated BMSCs *in vivo*, cells were labelled with CM-Dil before injection in tail vein. A greater number of CM-Dil-positive cells were observed in the im-BMSCs + SDF-1α-Hy group compared with the im-BMSCs group (Figure 5A-C), indicating that more transplanted BMSCs were recruited into the bone defects after local administration of SDF-1α. Immunofluorescence staining was performed to investigate the effect of SDF-1α delivery on osteogenesis *in vivo,* and showed that positive staining for Runx2 and OCN was notably stronger in new bone formation regions in the im-BMSCs + SDF-1α-Hy group compared with that in the im-BMSCs group

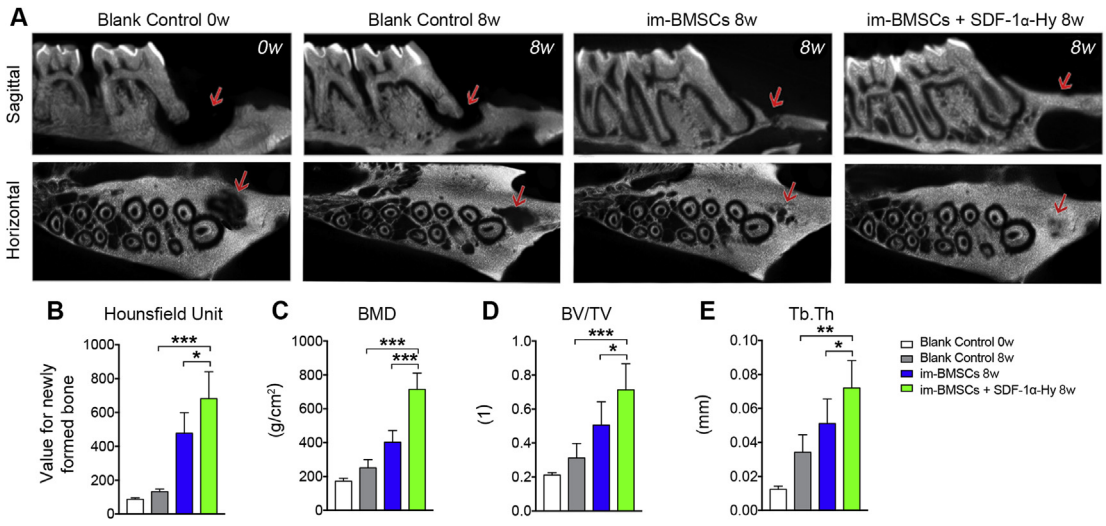

Figure 3. Micro-CT evaluation of *in vivo* bone formation. (A) Representative images of sagittal and horizontal section of micro-CT images at 8 weeks post-surgery. Red arrows, defect area. (B–E) Quantitative analysis of the volume of the newly formed bone by (B) HU, (C) BMD, (D) BV/TV and (E) Tb.Th in the defect area. Data are presented as mean ± SD. n = 5. $*p < 0.05$, $***p < 0.001$ represent significant differences.

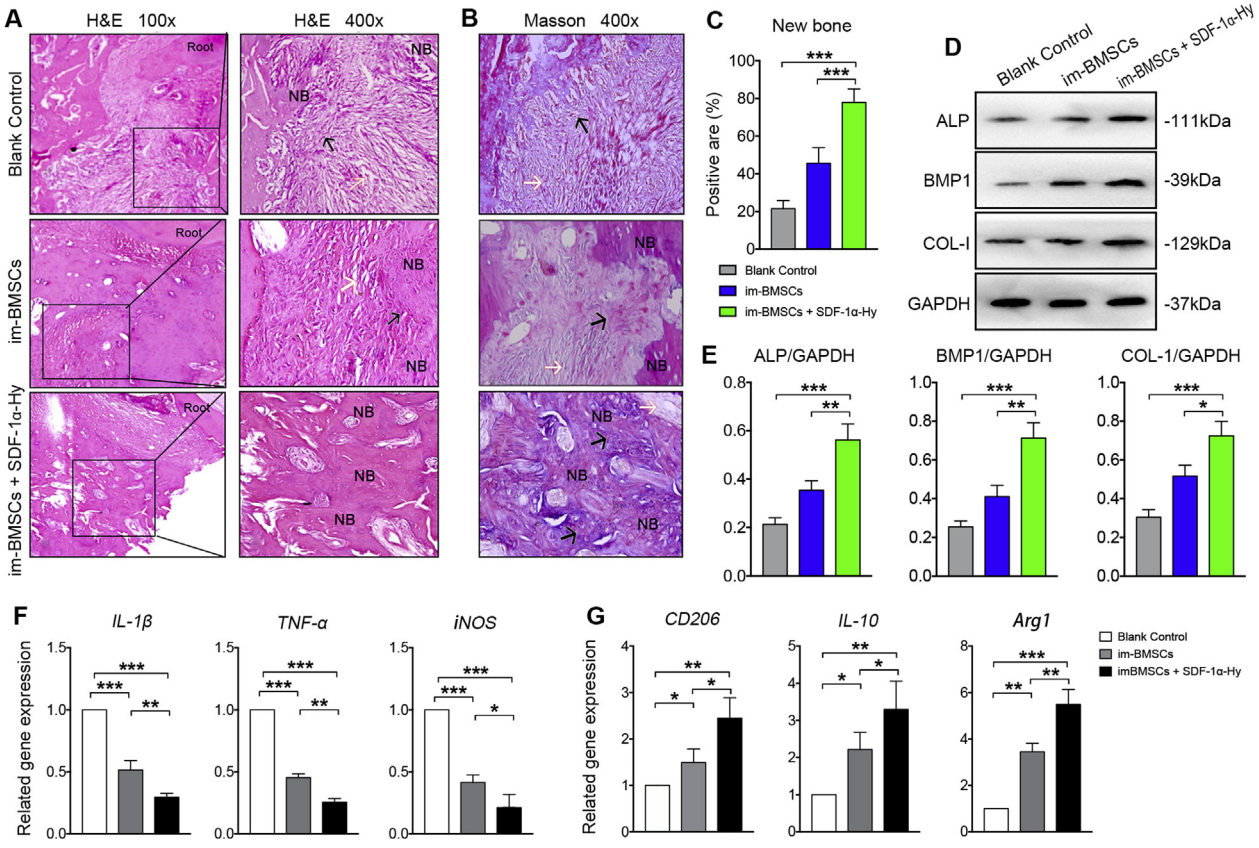

Figure 4. Histological analysis of newly formed bone and polarization states of macrophages in cervical lymph nodes. (A) Representative H&E staining images displaying the newly formed tissues *in vivo* at 8 weeks post-surgery. NB, newly formed bone. Root, the mesial root of first molar. The black arrows pointed to the primary bone tissues or bone trabecula-like tissues. The white arrows pointed to fibrous connective tissues. (B, C) Masson staining for the new bone and fibers and quantitative analysis. (D, E) Western blot for the related protein expression and its quantitation. (F, G) 8 weeks after transplantation, gene expression in cervical lymph nodes of IL-1β, TNF-α and iNOS (M1 phenotype-related) (F) and CD206, IL-10 and Arg1 (M2 phenotype-related) (G). Data are presented as mean ± SD. n = 5 for staining; n = 3 for qRT-PCR and western blot. $*p < 0.05$, $**p < 0.01$, $***p < 0.001$ represent significant differences.

(Fig. 5A, B, D). Further, there was more "Merged" cells of Runx2 and OCN with CM-Dil in the immunofluorescence staining of the im-BMSCs + SDF-1α-Hy group (Figure 5E). Consistent with the immunofluorescence results, the qRT-PCR analysis demonstrated that the mRNA expression of osteogenesis-related genes *Runx2* and *OCN* and the receptor of SDF-1α were significantly increased in the im-BMSCs + SDF-1α-Hy group compared with that in the im-BMSCs group (Figure 5F).

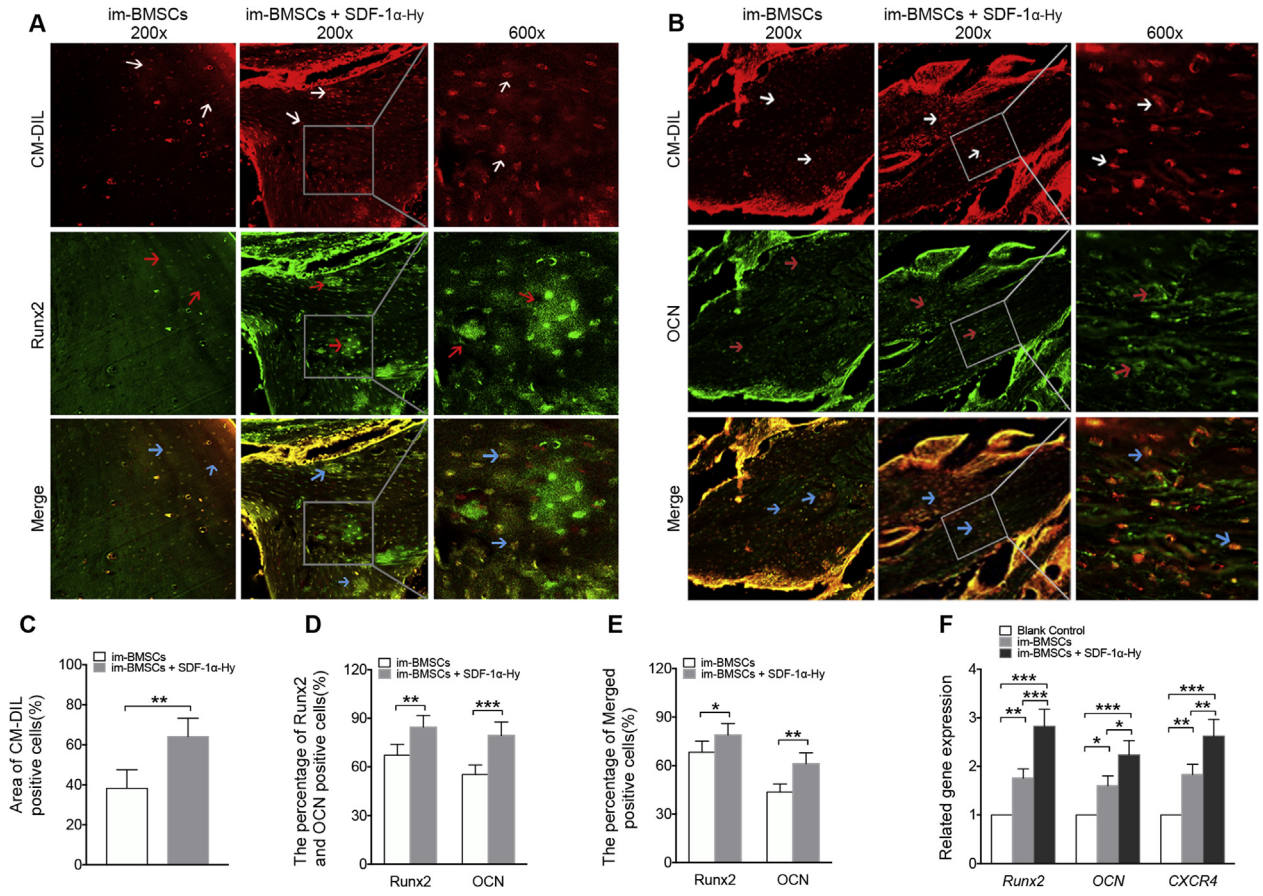

Figure 5. Representative immunofluorescent staining images for BMSCs recruitment and osteogenesis. (A) CM-Dil (red)/Runx2 (green) double staining of the newly formed tissues at 8 weeks post-surgery. White arrows, CM-Dil-labeled cells. Red arrows, Runx2-labeled cells. Blue arrows indicated both CM-Dil- and Runx2-labeled cells. (B) CM-DiI (red)/OCN (green) double staining of the newly formed tissues at 8 weeks post-surgery. White arrows indicated CM-DiI-labeled cells. Red arrows indicated OCN-labeled cells. Blue arrows indicated both CM-Dil- and OCN-labeled cells. (C) Quantitative analysis of the area ratio of CM-Dil-positive cells. (D) The percent of Runx2-and OCN-positive cells in the new bone formation regions. (E) Quantitative analysis of the Merged positive cells in A and B. (F) qRT-PCR analysis of *Runx2, Ocn* and *Cxcr4* genes in bone samples from the new bone formation regions. Data are presented as mean ± SD. n = 5 for immunofluorescent staining; n = 3 for qRT-PCR. *$p < 0.05$, **$p < 0.01$, ***$p < 0.001$ represent significant differences.

4. Discussion

MSCT therapy represents a promising approach for disease treatment and tissue regeneration, and numerous strategies have been applied to improve its efficacy for patients with osteoporosis. In this study, we proposed a novel strategy involving the use of SDF-1α application to enhance its therapeutic efficacy for osteoporotic bone healing.

Alveolar bone resorption is a common osteoporosis in post-menopausal women. Estrogen deficiency and the secondary onset of inflammation makes it difficult to treat bone defects with autologous BMSCs [23]. Systemic BMSCT presents a promising strategy for bone tissue engineering, while the shortcomings including poor engraftment of transplanted cells make it in relatively low efficacy [24]. Therefore, a large amount of exogenous cells is require to intravenously infuse into patients at one time [25], which might bring about a number of issues such as *ex-vivo* cell expansion and adverse effects induced by the infused BMSCs [26].

SDF-1α is a member of the CXC chemokine family, which is involved in numerous biological processes including cell migration and therapeutic stem cell homing [27]. In the cellular level, the SDF-1α works through its receptor CXCR4 to triggers the migration of CXCR4-positive stem cells and progenitor cells, such as BMSCs in regeneration of a variety of injured tissues and organs including bone [28]. Because of the short half-life and easy degradation of SDF-1α hydrogel, the use of this material in bone defect and tissue regeneration are still faced with challenges [29]. The CS/GP/HEC formulation enables sol-gel transition at 37 °C to achieve injectable *in situ* forming hydrogels, which can be simply injected into the body with endoscopy or percutaneous minimally invasive surgery [30]. In our study, the cumulative release of SDF-1α in CS/GP/HEC hydrogels demonstrated exceptionally high effect level about 96% at 21 d. Moreover, SDF-1α released from the hydrogels maintained its bioactivity to stimulate chemotaxis of BMSCs *in vitro*. This result is well consist with other studies which demonstrated that drug encapsulation such as insulin and doxorubicin hydrochloride into a CS/GP/HEC formulation allows a prolonged release [20, 31].

The micro-CT and histological analyses demonstrated that the release system of SDF-1α/CS/GP/HEC hydrogel enhanced the alveolar bone regeneration. Using BMSC tracing, we further demonstrated that cell recruitment of transplanted BMSCs to the defect site was successfully triggered through the localized and sustained release of SDF-1α from the hydrogels and hence the building of a special microenvironment for the osteogenic differentiation of BMSC. BMSCT combined with SDF-1α delivery could promote the expression of RUNX2 and OCN in the new bone regions through fluoresce staining. Consistently, qRT-PCR analysis indicated the local administration of SDF-1α could increase the gene expression of *Runx2* and *Ocn in vivo*.

During the initial process of regeneration, the damaged tissues sent out a series of signals which mediated healing to direct reparative cells to the injured tissues [32]. SDF-1α/CXCR4 signaling plays a pivotal role in the regulation of BMSCs homing and the engraftment of transplanted

BMSCs for the design of innovative biomaterials and therapies to achieve regeneration of damaged tissues [27]. Analogously, local administration of SDF-1α has a stimulatory effect on stem cell recruitment to promote osteointegration of titanium implants in rat tibia [33]. Moreover, some researchers attempted to improve stem cell therapy by overexpressing *Sdf-1α* or *Cxcr4* gene of BMSCs before transplantation [34, 35]. According to our previous work basis [5], SDF-1α-mediated migration of both Sham- and OVX-BMSCs is related to the PI3K/AKT signaling pathway. Our Recent studies uncover a novel mechanism by sustained release SDF-1α to recruit BMSCs. Furthermore, we observed more vascular structures and higher expression of *Cxcr4* gene in the newly formed tissue after SDF-1α delivery compared with BMSC transplantation alone. Although the contribution of *in vivo* stem and progenitor cells recruitment to the bone defect area was not confirmed in our study, these results indicated that local administration of SDF-1α might recruit other CXCR4-positive cells such as hematopoietic stem cells and endothelial progenitor cells which are responsible for angiogenesis. The neovascularization could facilitate oxygen and nutrition supply for reparative cells and hence indirectly enhance bone formation.

In recent years, the modulation of macrophage behavior has excellent benefit for the tissue regeneration and therapeutic methods [36]. Some researchers found that the use of drug-delivery system for the sustaining release of SDF-1α could collect the regenerative cells including anti-inflammatory monocytes and M2 macrophages in tissues [37]. In our study, decreased expression of pro-inflammatory (M1) cytokines like *TNF-α*, *iNOS* and *IL-1β* as well as enhanced expression of the anti-inflammatory (M2) cytokines like *Arg1*, *CD206* and *IL-10* was observed after local administration of SDF-1α compared with BMSC transplantation alone. Similarly, the fibrous films which promoted M1 stage to M2 stage of macrophage, could enhance the release of SDF-1α in the hydrogel and increase the recruitment of BMSC [38]. Although we revealed that local administration of SDF-1α promoted macrophage polarization toward the M2 phenotype, further studies are needed to investigate whether SDF-1α has a direct regulatory effect on the macrophage polarization.

Collectively, we have demonstrated that local SDF-1α application had beneficial effects in BMSCT therapy for osteoporotic bone healing by facilitating stem cell recruitment, regulating macrophage polarization and promoting osteogenesis *in vivo*. Our findings suggest that targeting SDF-1α long-term transplantation is a potential therapeutic strategy for the treatment of osteoporosis.

Declarations

Author contribution statement

H. Yang: Conceived and designed the experiments; Wrote the paper.

Q. Liu: Conceived and designed the experiments; Performed the experiments; Analyzed and interpreted the data; Wrote the paper.

Y. Wen: Performed the experiments; Analyzed and interpreted the data.

J. Qiu and Z. Zhang: Performed the experiments.

Z. Jin: Contributed reagents, materials, analysis tools or data.

M. Cao: Analyzed and interpreted the data.

Y. Jiao: Conceived and designed the experiments.

Funding statement

This work was supported by the National Natural Science Foundation of China (No. 81500867 and No. 81970960); and the Open Project of State Key Laboratory of Military Stomatology (No. 2018KA02 and No. 2018MZ01).

Competing interest statement

The authors declare no conflict of interest.

Additional information

No additional information is available for this paper.

References

[1] B.L. Foster, M. Ao, C. Willoughby, Y. Soenjaya, E. Holm, L. Lukashova, et al., Mineralization defects in cementum and craniofacial bone from loss of bone sialoprotein, Bone 78 (2015) 150–164.

[2] L. Xia, Z. Yin, L. Mao, X. Wang, J. Liu, X. Jiang, et al., Akermanite bioceramics promote osteogenesis, angiogenesis and suppress osteoclastogenesis for osteoporotic bone regeneration, Sci. Rep. 6 (2016) 22005.

[3] C.H. Chen, L. Wang, U.S. Tulu, M. Arioka, M.M. Moghim, B. Salmon, et al., An osteopenic/osteoporotic phenotype delays alveolar bone repair, Bone 112 (2018) 212–219.

[4] Y.X. He, G. Zhang, X.H. Pan, Z. Liu, L Zhen Zheng, C.W. Chan, et al., Impaired bone healing pattern in mice with ovariectomy-induced osteoporosis: a drill-hole defect model, Bone 48 (2011) 1388–1400.

[5] Q. Liu, X. Zhang, Y. Jiao, X. Liu, Y. Wang, S.L. Li, et al., In vitro cell behaviors of bone mesenchymal stem cells derived from normal and postmenopausal osteoporotic rats, Int. J. Mol. Med. 41 (2018) 669–678.

[6] G.Q. Daley, D.T. Scadden, Prospects for stem cell-based therapy, Cell 132 (2008) 544–548.

[7] A.C. Vural, S. Odabas, P. Korkusuz, A.S. Yar Sağlam, E. Bilgiç, T. Çavuşoğlu, et al., Cranial bone regeneration via BMP-2 encoding mesenchymal stem cells, Artif. Cells Nanomed. Biotechnol. 45 (2017) 544–550.

[8] I.M. Barbash, P. Chouraqui, J. Baron, M.S. Feinberg, S. Etzion, A. Tessone, et al., Systemic delivery of bone marrow-derived mesenchymal stem cells to the infarcted myocardium: feasibility, cell migration, and body distribution, Circulation 108 (2003) 863–868.

[9] T. Yamaza, Y. Miura, Y. Bi, Y. Liu, K. Akiyama, W. Sonoyama, et al., Pharmacologic stem cell based intervention as a new approach to osteoporosis treatment in rodents, PloS One 3 (2008), e2615.

[10] F. Taraballi, G. Bauza, P. McCulloch, J. Harris, E. Tasciotti, Concise review: biomimetic functionalization of biomaterials to stimulate the endogenous healing process of cartilage and bone tissue, Stem Cells Transl. Med. 6 (2017) 2186–2196.

[11] D.J. Mooney, H. Vandenburgh, Cell delivery mechanisms for tissue repair, Cell Stem Cell 2 (2008) 205–213.

[12] T.T. Lau, D.A. Wang, Stromal cell-derived factor-1 (SDF-1): homing factor for engineered regenerative medicine, Expet Opin. Biol. Ther. 11 (2011) 189–197.

[13] A. Dar, O. Kollet, V. Shinder, P. Goichberg, A. Kalinkovich, M. Zsak, et al., CXCR4-dependent internalization and secretion of functional SDF-1 by bone marrow endothelial and stromal cells, Exp. Hematol. 33 (2005) 118.

[14] Y. Kawakami, M. Ii, T. Matsumoto, R. Kuroda, T. Kuroda, S.M. Kwon, et al., SDF-1/CXCR4 axis in tie2-Lineage cells including endothelial progenitor cells contributes to bone fracture healing, J. Bone Miner. Res. 30 (2015) 95–105.

[15] W. Ji, F. Yang, J. Ma, M.J. Bouma, O.C. Boerman, Z. Chen, et al., Incorporation of stromal cell-derived factor-1α in PCL/gelatin electrospun membranes for guided bone regeneration, Biomaterials 34 (2013) 735–745.

[16] K. Hatano, Y. Ishida, H. Yamaguchi, J. Hosomichi, J Ichi Suzuki, R. Usumi-Fujita, et al., The chemokine receptor type 4 antagonist, AMD3100, interrupts experimental tooth movement in rats, Arch. Oral Biol. 86 (2018) 35–39.

[17] H.Y. Zhou, L.J. Jiang, P.P. Cao, J.B. Li, X.G. Chen, Glycerophosphate-based chitosan thermosensitive hydrogels and their biomedical applications, Carbohydr. Polym. 117 (2015) 524–536.

[18] Y. Wen, H. Yang, Y. Liu, Q. Liu, A. Wang, Y. Ding, et al., Evaluation of BMMSCs-EPCs sheets for repairing alveolar bone defects in ovariectomized rats, Sci. Rep. 7 (2017) 16568.

[19] L. Wen, Y. Wang, N. Wen, G. Yuan, M. Wen, L. Zhang, et al., Role of endothelial progenitor cells in maintaining stemness and enhancing differentiation of mesenchymal stem cells by indirect cell-cell interaction, Stem Cell. Dev. 25 (2016) 123–138.

[20] H. Naderi-Meshkin, K. Andreas, M.M. Matin, M. Sittinger, H.R. Bidkhori, N. Ahmadiankia, et al., Chitosan-based injectable hydrogel as a promising in situ forming scaffold for cartilage tissue engineering, Cell Biol. Int. 38 (2014) 72–84.

[21] Y. Wen, H.X. Yang, J.J. Wu, A.X. Wang, X.D. Chen, S.J. Hu, et al., COL4A2 in the tissue-specific extracellular matrix plays important role on osteogenic differentiation of periodontal ligament stem cells, Theranostics 9 (2019) 4265–4286.

[22] J. Zhao, Y. Yan, X. Huang, L.Q. Sun, Y.P. Li, Therapeutic effects of VEGF gene-transfected BMSCs transplantation on thin endometrium in the rat model, Stem Cell. Int. 2018 (2018) 3069741.

[23] B.D. Sui, C.H. Hu, C.X. Zheng, Y. Shuai, X.N. He, P.P. Gao, et al., Recipient glycemic micro-environments govern therapeutic effects of mesenchymal stem cell infusion on Osteopenia, Theranostics 7 (2017) 1225–1244.

[24] N. Liu, J. Tian, J. Cheng, J. Zhang, Migration of CXCR4 gene-modified bone marrow-derived mesenchymal stem cells to the acute injured kidney, J. Cell. Biochem. 114 (2013) 2677–2689.

[25] K. Le Blanc, F. Frassoni, L. Ball, F. Locatelli, H. Roelofs, I. Lewis, et al., Mesenchymal stem cells for treatment of steroid-resistant, severe, acute graft-versus-host disease: a phase II study, Lancet 371 (2008) 1579–1586.

[26] P.R. Vulliet, M. Greeley, S.M. Halloran, K.A. MacDonald, M.D. Kittleson, Intra-coronary arterial injection of mesenchymal stromal cells and microinfarction in dogs, Lancet 363 (2004) 783–784.

[27] X. Li, X.T. He, Y. Yin, R.X. Wu, B.M. Tian, F.M. Chen, Administration of signalling molecules dictates stem cell homing for in situ regeneration, J. Cell Mol. Med. 21 (2017) 3162–3177.
[28] A. Cipitria, K. Boettcher, S. Schoenhals, D.S. Garske, K. Schmidt-Bleek, A. Ellinghaus, et al., In-situ tissue regeneration through SDF-1α driven cell recruitment and stiffness-mediated bone regeneration in a critical-sized segmental femoral defect, Acta Biomater. 60 (2017) 50–63.
[29] V.F.M. Segers, T. Tokunou, L.J. Higgins, C. MacGillivray, J. Gannon, R.T. Lee, Local delivery of protease-resistant stromal cell derived factor-1 for stem cell recruitment after myocardial infarction, Circulation 116 (2007) 1683–1692.
[30] A.A. Amini, L.S. Nair, Injectable hydrogels for bone and cartilage repair, Biomed. Mater. 7 (2012) 24105.
[31] J. Wu, Z.G. Su, G.H. Ma, A thermo- and pH-sensitive hydrogel composed of quaternized chitosan/glycerophosphate, Int. J. Pharm. 315 (2006) 1–11.
[32] R.X. Wu, X.Y. Xu, J. Wang, X.T. He, H.H. Sun, F.M. Chen, Biomaterials for endogenous regenerative medicine: coaxing stem cell homing and beyond, Appl. Mater. Today 15 (2018) 71.
[33] J. Karlsson, N. Harmankaya, A. Palmquist, S. Atefyekta, O. Omar, P. Tengvall, et al., Stem cell homing using local delivery of plerixafor and stromal derived growth factor-1alpha for improved bone regeneration around Ti-implants, J. Biomed. Mater. Res. A 104 (2016) 2466–2475.
[34] C.Y. Ho, A. Sanghani, J. Hua, M. Coathup, P. Kalia, G. Blunn, Mesenchymal stem cells with increased stromal cell-derived factor 1 expression enhanced fracture healing, Tissue Eng. A 21 (2015) 594–602.
[35] S.W. Cho, H.J. Sun, J.-Y. Yang, J.Y. Jung, J.H. An, H.Y. Cho, et al., Transplantation of mesenchymal stem cells overexpressing RANK-Fc or CXCR4 prevents bone loss in ovariectomized mice, Mol. Ther. 17 (2009) 1979–1987.
[36] T.A. Wynn, K.M. Vannella, Macrophages in tissue repair, regeneration, and fibrosis, Immunity 44 (2016) 450–462.
[37] J.R. Krieger, M.E. Ogle, J. McFaline-Figueroa, C.E. Segar, J.S. Temenoff, E.A. Botchwey, Spatially localized recruitment of anti-inflammatory monocytes by SDF-1α-releasing hydrogels enhances microvascular network remodeling, Biomaterials 77 (2016) 280–290.
[38] Q. Zhang, J.W. Hwang, J.H. Oh, C.H. Park, S.H. Chung, Y.S. Lee, et al., Effects of the fibrous topography-mediated macrophage phenotype transition on the recruitment of mesenchymal stem cells: an in vivo study, Biomaterials 149 (2017) 77–87.